Published by :
http://www.ijert.org

International Journal of Engineering Research & Technology (IJERT)
ISSN: 2278-0181
Vol. 9 Issue 04, April-2020

Design and Implementation of Z Source Resonant Converter for EV Wire Less Charging Application

Athira Rajan
PG Student
Electrical and Electronics Engineering
NSS College of Engineering
Kerala, India

Jithin Kumar I J
Assistant Professor
Electrical and Electronics Engineering
GEC Palakkad
Kerala, India

Abstract — **Wireless Power Transfer (WPT) technology is an emerging research area due to its safety and convenience. A Conventional WPT system has Front End PFC and DC-DC Boost Converter which makes the system bulkier. The Z Source Inverter (ZSI) was introduced into WPT systems to improve the system performance. The ZSI regulates the input voltage in WPT systems without Front End Converters and makes the inverter bridge immune to Shoot Through (ST) states. The results are through simulations and Finally, the designed system is implemented experimentally**

I. INTRODUCTION

WPT technology deliver power through an electromagnetic field without any physical connection between the transmitter and receiver [1]-[3]. Recent advancements in this field have led to more stringent design requirements being proposed and studied by researchers, such as efficiency improvement [4]-[8], coupling variation [9], [10], foreign object detection [11], [12], and output regulation [13]-[15]. Electronic technology plays a crucial role in these research studies and spurs WPT technology development. The voltage source inverter (VSI) is an essential part of a WPT system that generates high-frequency ac power for transmission across a wireless media. Unfortunately, the output voltage of conventional VSI is always is equal to or lower than the input voltage, which limits this inverter's application in small-voltage or wide input situations. To address this barrier, front-end converters, such as boost converter or buck-boost converter are inserted between a dc source and a VSI to boost the dc-rail voltage [16], [17]. However, this require more space and increase the cost of the system. To add one additional IGBT/MOSFET one extra heat sink and associated drive circuitry is to be accommodated. Considering the incremental cost and design complications, the ZSI presents a better alternative to front-end converters in WPT system.

When compared with a conventional VSI, the ZSI has an input diode DS and a Z-source network added between the dc voltage source and the VSI [18]. The Z-source network consists of two identical inductors (L1 and L2) and capacitors (C1 and C2) to boost the output voltage by shorting one or two legs of the rear-end inverter bridge. This is also referred to as the shoot-through (ST) state.

Guidelines to design Z-source network based on steady state parameters were presented in [19]. Since the network is connected to a three-phase VSI, the output current of the network is regarded as a constant current. Meanwhile, the current in the network of WPT system is approximately sinusoidal over part of one switching period due to a sinusoidal resonant current. The mathematical analysis in [19] is modified when applied to a WPT system. In [20], the benefits of a ZSI in resonant converters are analyzed. These benefits include improved robustness and reliability, buck/boost function, and high efficiency over wide input and load ranges.

The ZSN in the proposed ZSRI provides the unique feature of inherent power factor correction (PFC) without adding extra switching devices. It is possible because it adds the unique features of immunity to the H-bridge inverter during shoot-through states. This characteristic makes the input current as a sinusoidal waveform and in phase with the ac input voltage. This variable also provides a boost factor to the system. However, to regulate the output voltage, the proposed ZSN-based inverter uses the active state duty cycle, which is a common control variable used in series resonant inverters. Both control variables are used in the series resonant H-bridge inverter and the ZSRI does not require additional control circuitry to provide power factor correction. In other words, because of the ZSN, the ZSRI can perform power factor correction as well as dc/ac conversion in single stage.

II. OPERATION OF Z SOURCE RESONANT CONVERTER

The ZSRC has more states in one switching cycle compared with other DC- AC systems. It is important to clarify all these states to understand the ZSRC. The boost ratio of ZSN is still related to the total shoot-through state duty cycle among these states. The operation principle of the ZSRC is described based here with an example of the phase-shift control method. Assuming that the ZSN is symmetrical ($C_1 = C_2 = C$, and $L_1 = L_2 = L$) therefore, $V_{C1} = V_{C2} = VC$, and $V_{C1} = V_{C2} = V_C$. Also, the resonant frequency of L and C in ZSN is at least ten times smaller than the switching frequency. Hence, the ZSN inductor current and the ZSN capacitor voltage are considered to be constant in one switching cycle. Fig. 2 shows the conducting devices in different states—active state, shoot through state, and zero state.

International Journal of Engineering Research & Technology (IJERT)
ISSN: 2278-0181
Vol. 9 Issue 04, April-2020

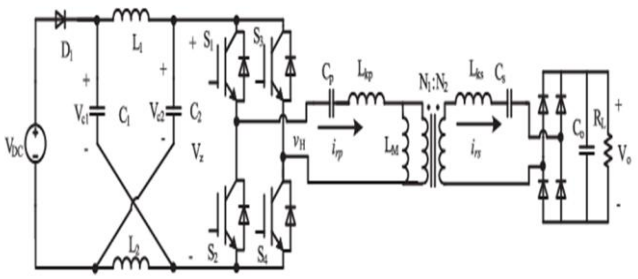

Fig 1. Circuit of WPT System with a ZSI

1. ***Active State***: During the two active states time interval [see Fig. 6(c) and (g)], the diagonal switches are on, and the input side diode D1 is conducting. The resonant network draws current from both the ZSN inductor and capacitor. The difference between load current and ZSN inductor current is provided by a series connection of the two ZSN capacitor and dc source. The current going through the switches are only load current The ZSN inductor voltage for this time interval is given as

$$V_L = V_{DC} - V_C$$

2. ***Shoot-Through State:*** Three of the switches are ON. The two horizontal switches are carrying the load current and the switches in one-phase leg are carrying the ZSN inductor current. Hence, there is one switch carrying the sum of the two currents. Since the flow of ZSN inductor current is always in one direction and the load current would be bipolar, these two currents either subtract from each other or add together, contributing to the sum with their absolute value. Fortunately, phase-shift control only allows different polarity currents going through the same switch in shoot-through state. Here, the ZSN capacitors will charge ZSN inductors (this is how the ZSRC can boost the voltage). The ZSN inductor voltage for this time interval is given as

$$V_L = V_C$$

3. ***Zero State***: During the zero state's time interval, two horizontal switches are ON. The ZSN is isolated from the load. The load current is freewheeling and the ZSN inductors charge the ZSN capacitors. The ZSN inductors voltage for this time interval is given as

$$V_L = V_{DC} - V_C$$

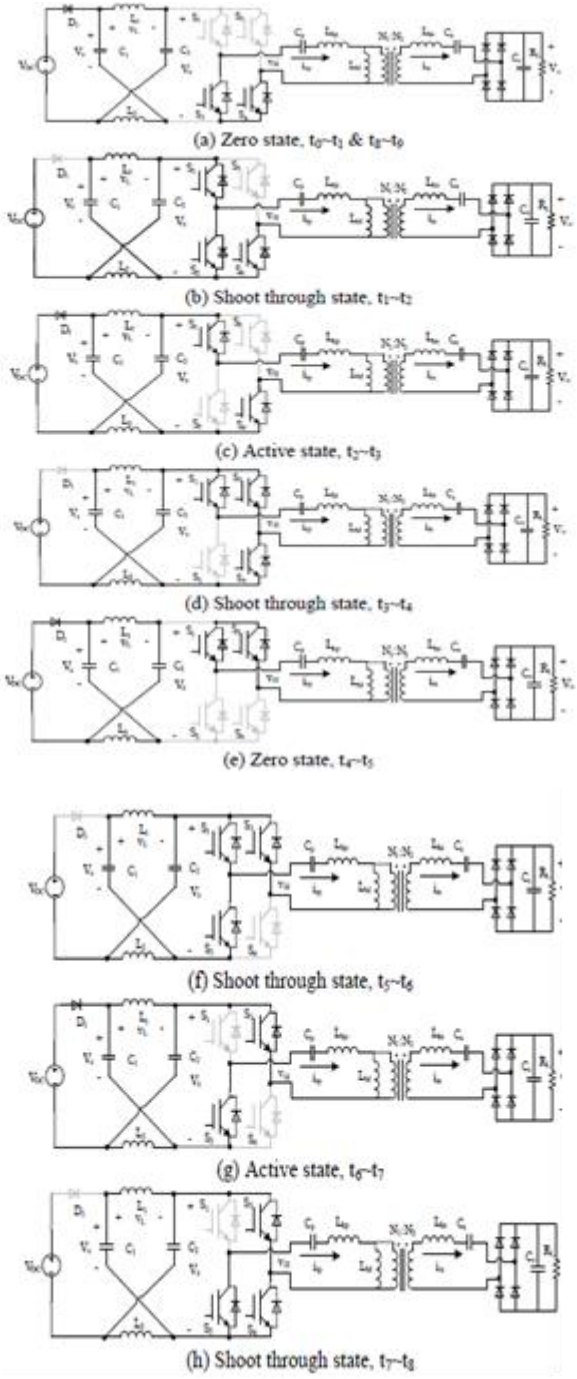

Fig 2. ZSRC circuit diagram in different states

These three states are all the possible states in ZSRC. Different allocation of these three states along one switching period would generate different load regulation characteristic.

International Journal of Engineering Research & Technology (IJERT)
ISSN: 2278-0181
Vol. 9 Issue 04, April-2020

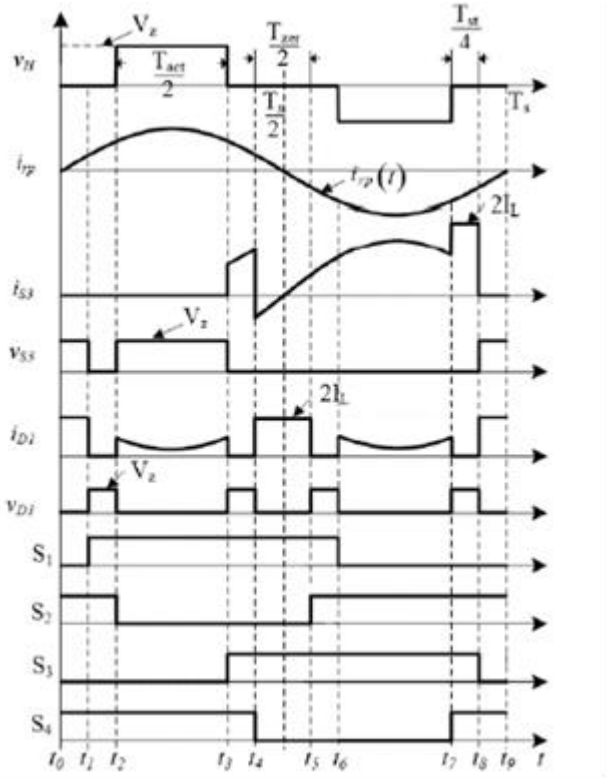

Fig 3. Time domain waveforms for phase shift control in ZSRC

III. SIMULATION OF WPT SYSTEM WITH ZSI

Simulation of Z Source Resonant Converter for EV Wireless Charging is done using MATLAB/Simulink 2016

1. Simulation Parameters

Simulation parameters are shown in table 1.

TABLE 1

Input Voltage	12 V
Resonant Frequency	20 kHz
Transformer Turns Ratio	20 : 15
ZSN Capacitors	4.7mF
ZSN Inductor	1mH
Output Filter Capacitor	1mF
Primary Side Leakage Inductance	0.415mH
Secondary Side Leakage Inductance	1.07mH
Primary Side Leakage Capacitance	180nF
Secondary Side Leakage Capacitance	65.8nF

The input voltage of the ZSRC is Vs=33V and the output voltage and current is Vo=88v and Io=2.28A with the resonant frequency of 20kHZ. Assuming that the ZSN is symmetrical ($C_1 = C_2 = C$, and $L_1 = L_2 = L$) therefore, $V_{C1} = V_{C2} = V_C$, and $V_{L1} = V_{L2} = V_L$. Also, the resonant frequency of L and C in ZSN is at least ten times smaller than the switching frequency. Hence, the ZSN inductor current and the ZSN capacitor voltage are constant in one switching cycle.

The significant part of the design is choosing the inductor and capacitor values and operating frequency. On the contrary, use of the low frequency leads to increases both on the size and also the cost of inductors and capacitors. Thus, there is a trade-off between the size and efficiency in determining the operating frequency of the converter. The frequency is selected as 20kHz.

2. Simulation Result

The complete model of the developed WPT is shown in Fig.4

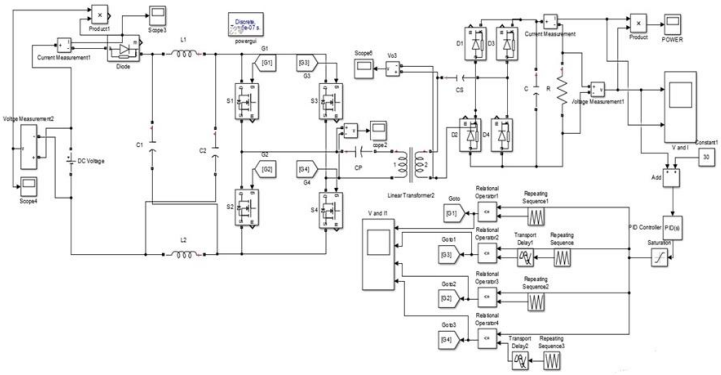

Fig 4. Simulation Diagram of ZSRC for WPT

Simulation has been performed and the results are presented for each converter stage. The circuit consists of a high frequency (HF) Z Source Resonant Converter. High frequency switching is implemented using MOSFET switches. This is the high frequency link. A HF transformer provides voltage transformation and isolation between the DC source and the load. At the output side, a full bridge rectifier is connected to load. For analytical study, a resistive load is selected. The closed loop is controlled for constant output.

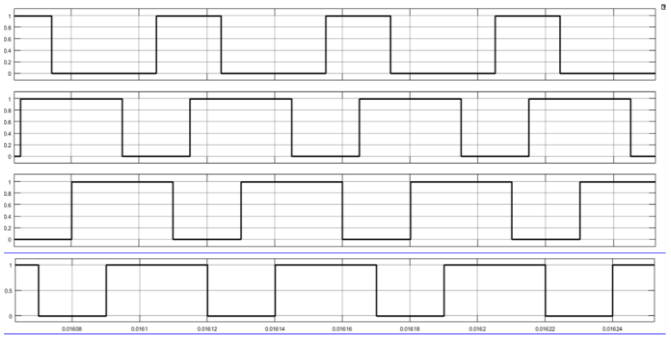

Fig 5. Waveform of Gating signal for MOSFETS

International Journal of Engineering Research & Technology (IJERT)
ISSN: 2278-0181
Vol. 9 Issue 04, April-2020

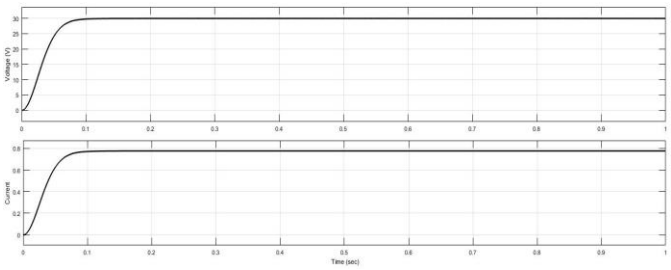

Fig 6. Waveform of output voltage and output current of the ZSRC

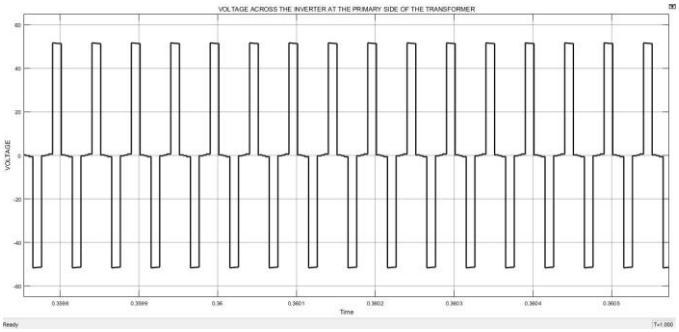

Fig 7. Voltage across the H bridge at the primary side

IV. HARDWARE IMPLEMENTATION

The main circuit diagram consists of four sections, converter section, control section, driver section and power circuit. The converter section consists of four IRFP460N MOSFETs. Even if there is any fluctuations in the input the output will be maintained constant by the program stored in the microcontroller. Microcontroller sends the corresponding signals which will be too feable to drive the MOSFET switches, so a driver circuit consisting of TLP250 Driver are used which boosts the amplitude of the signals enough to drive the switches.

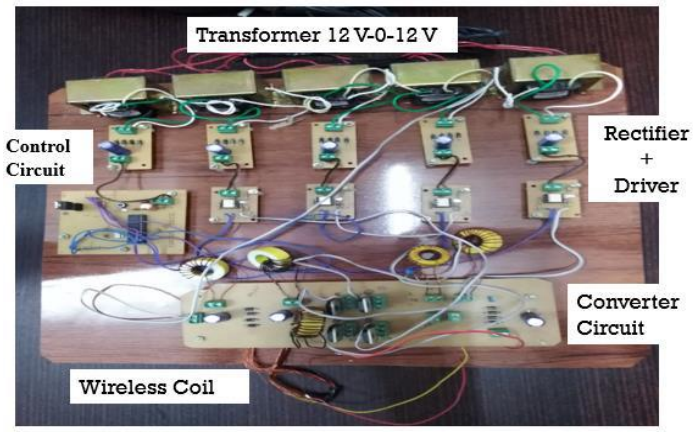

Fig 8 Complete Hardware Setup

Fig 9 Wireless Power Transfer Setup

Fig 10 Output Obtained

V. CONCLUSION

A new circuit topology for high power WPT applications using a full bridge Z-source resonant inverter has been developed and simulated. The control methods in the system with the insertion of shoot-through modes of the Z-source inverter have been investigated. In simulation, ideal MOSFETs and diodes were used. The output voltage of 27 V and output current of 0.9 A, i.e output of 23.5 W is obtained for the coupling coefficient k of 0.2. In the experiment, an output current of 0.9 A, and output voltage of 16 V was obtained. The slight difference between the simulation and experimental results is due to the following reasons: Core losses, simulation-ideal diode and MOSFET switches were used. Nevertheless, in both the simulation and experiment, the results obtained are very close to the analytical design value. This, in turn, validates the designed parameters.

VI. REFERENCES

[1] A. Kurs, A. Karalis, R. Moffatt, J. D. Joannopoulos, P. Fisher, and M. Soljacic, "Wireless power transfer via strongly coupled magnetic resonances," *Science*, Vol. 317, pp. 83-86, Jul. 2007.

[2] J. T. Boys and G. A. Covic, "The Inductive Power Transfer Story at the University of Auckland," *IEEE Circuits Syst. Mag*., Vol. 15, No.2, pp. 6-27, May 2015

[3] H. Vázquez-Leal, A. Gallardo-Del-Angel, and R. Castañeda-Sheissa, "The Phenomenon of Wireless Energy Transfer: Experiments and Philosophy," in *Wireless Power Transfer-Principles and Engineering Explorations, InTech*, Chap. 1, pp. 1-18, 2012.

[4] R. Melki and B. Moslem, "Optimizing the design parameters of a wireless power transfer system for maximizing power transfer efficiency: A simulation study," in *Technological Advances in Electrical, Electronics and Computer Engineering (TAEECE)*, pp. 278-282, 2015

[5] X. Wang, H. Zhang, and Y. Liu, "Analysis on the efficiency of magnetic resonance coupling wireless charging for electric

International Journal of Engineering Research & Technology (IJERT)
ISSN: 2278-0181
Vol. 9 Issue 04, April-2020

vehicles," in *Cyber Technology in Automation, Control and Intelligent Systems (CYBER)*, pp. 191-194, 2013.

[6] B. Kallel, O. Kanoun, T. Keutel, and C. Viehweger, "Improvement of the efficiency of MISO configuration in inductive power transmission in case of coils misalignment," in *Instrumentation and Measurement Technology Conference (I2MTC) Proceedings*, pp. 856-861, 2014.

[7] M. Fu, T. Zhang, C. Ma, and X. Zhang, "Efficiency and Optimal Loads Analysis for Multiple-Receiver Wireless Power Transfer Systems," *IEEE Trans. Microw. Theory Techn.*, Vol. 63, No. 3, pp. 801-812, Mar. 2015.

[8] Z. Low, R. Chinga, R. Tseng, and J. Lin, "Design and test of a high-power high-efficiency loosely coupled planar wireless power transfer system," *IEEE Trans. Ind. Electron.*, Vol. 56, No. 5, pp. 1801-1812, May 2009.

[9] O. Jonah, S. V. Georgakopoulos, D. Daerhan, and Y. Shun, "Misalignment-insensitive wireless power transfer via strongly coupled magnetic resonance principles," in *Antennas and Propagation Society International Symposium (APSURSI)*, pp. 1343-1344, 2014.

[10] H. Feng, T. Cai, S. Duan, J. Zhao, X. Zhang, and C. Chen, "An LCC-compensated resonant converter optimized for robust reaction to large coupling variation in dynamic wireless power transfer," *IEEE Trans. Ind. Electron.*, Vol. 63, No. 10, pp. 6591-6601, Oct. 2016.

[11] N. Kuyvenhoven, C. Dean, J. Melton, J. Schwannecke, and A. Umenei, "Development of a foreign object detection and analysis method for wireless power systems," in *Product Compliance Engineering (PSES) Proceedings*, pp. 1-6, 2011

[12] G. Jang, S. Jeong, H. Kwak, and C. Rim, "Metal object detection circuit with non-overlapped coils for wireless EV chargers," in *Southern Power Electronics Conference (SPEC)*, pp. 1-6, 2016.

[13] L. Tan, S. Pan, C. Xu, C. Yan, H. Liu, and X. Huang, "Study of constant current-constant voltage output wireless charging system based on compound topologies," *J. Power Electron.*, Vol. 17, No. 4, pp. 1109-1116, Jul. 2017.

[14] L. Sun, H. Tang, and C. Yao, "Investigating the frequency for load-independent output voltage in three-coil inductive power transfer system," *Int. J. Circ. Theor. Appl*, Vol. 44, No. 6, pp. 1341-1348, Aug. 2015

[15] L. Zhang, X. Yang, W. Chen, and X. Yao, "An isolated soft-switching bidirectional buck-boost inverter for fuel cell applications," *J. Power Electron.*, Vol. 10, No. 3, pp. 235-244, May 2010.

[16] R. Mosobi, T. Chichi, and S. Gao, "Modeling and power quality analysis of integrated renewable energy system," in *National Power Systems Conference (NPSC)*, pp. 1-6, 2014

[17] F. Peng, "Z-source inverter," *IEEE Trans. Ind. Appl.*, Vol. 39, No. 2, pp. 504-510, Mar. 2003.

[18] S. Rajakaruna and L. Jayawickrama, "Steady-state analysis and designing impedance network of z-source inverters," *IEEE Trans. Ind. Electron., Vol*. 57, No. 7, pp. 2483-2491, Jul. 2010.

[19] H. Cha, F. Peng, and D. Yoo, "Z-source resonant DC-DC converter for wide input voltage and load variation," in *Power Electronics Conference (IPEC)*, pp. 995-1000, 2010.

[20] H. Zeng and F. Z. Peng, "SiC based z-source resonant converter with constant frequency and load regulation for EV wireless charger," *IEEE Trans. Power Electron.*, Vol. 32, No. 11, pp. 8813-8822, Nov. 2017.

[21] T. Wang, X. Liu, H. Tang, and M. Ali, "Modification of the wireless power transfer system with Z-source inverter," *IET Electron. Letters*, Vol. 53, No. 2, pp. 106-108, Jan. 2017.